Journal of Inflammation Research

Dovepress
Taylor & Francis Group

Open Access Full Text Article

ORIGINAL RESEARCH

Development and Validation of a CTE-Based Radiomics Nomogram for Predicting Clinical Adverse Outcomes in Patients with Stricturing Crohn's Disease

Bo Zhang[1,*], Yankun Gao[1,*], Li Tong[2], Jing Hu[3], Xingwang Wu[1]

[1]Department of Radiology, The First Affiliated Hospital of Anhui Medical University, Hefei, Anhui, 230022, People's Republic of China; [2]Department of Radiology, The Third Affiliated Hospital of Anhui Medical University, Hefei, Anhui, 230061, People's Republic of China; [3]Department of Gastroenterology, The First Affiliated Hospital of Anhui Medical University, Hefei, Anhui, 230022, People's Republic of China

*These authors contributed equally to this work

Correspondence: Xingwang Wu, Department of Radiology, The First Affiliated Hospital of Anhui Medical University, Hefei, Anhui, 230022, People's Republic of China, Email duobi2004@126.com

Objective: This study sought to develop and validate a radiomics nomogram using computed tomography enterography (CTE) to predict clinical adverse outcomes (CAO) in patients with stricturing Crohn's disease (CD), aiding in personalized treatment planning.
Methods: We retrospectively collected data from 219 patients diagnosed with stricturing CD between January 2018 and March 2023 at our institution, dividing them into a training set (n=153) and a testing set (n=66). Radiomics features from strictured segments were extracted and the most predictive features were identified using Pearson correlation, SelectKBest, and Least Absolute Shrinkage and Selection Operator (LASSO) regression to derive a Radiomics score (Rad-score). Cox regression was used to select key clinical predictors of CAO. A radiomics nomogram was developed to predict CAO, evaluated using Harrell's concordance index (C-index), time-dependent Receiver Operating Characteristic (ROC) curves, and Decision Curve Analysis (DCA).
Results: Univariate and multivariate Cox regression analyses of the training set identified the HBI score (HR=0.443, 95% CI=0.212–0.925, P=0.030) and the diameter of the upstream lumen (HR=1.080, 95% CI=1.050–1.111, P<0.001) as independent clinical predictors of CAO in stricturing CD. Nineteen features related to CAO outcomes were selected for Rad-score calculation. In the testing set, the C-index for the clinical, radiomics, and nomogram models were 0.752, 0.775, and 0.849, respectively. The AUCs of the nomogram model at 1, 2, and 3 years were 0.874, 0.863, and 0.956, respectively.
Conclusion: The CTE-based radiomics nomogram significantly outperformed clinical and radiomics models alone and demonstrated excellent predictive accuracy for CAO risk. By integrating the HBI score and upstream lumen diameter with radiomics features, this tool provides clinicians with a validated, noninvasive method to stratify stricturing CD patients by risk and guide personalized therapeutic decisions.

Keywords: radiomics, computed tomography enterography, Crohn's disease, outcomes

Introduction

Crohn's disease (CD) is a chronic inflammatory bowel disease (IBD) that presents complex challenges in both diagnosis and treatment.[1,2] The Montreal classification sorts CD into non-stricturing non-penetrating, stricturing, and penetrating types.[3,4] At diagnosis, approximately half of the patients exhibit intestinal strictures, primarily in the small intestine, which, if left untreated, may progress to obstructive or penetrating disease, increasing the risk of disability.[5–9] Intestinal strictures in CD can be inflammatory, fibrotic, or mixed. Intestinal stenosis treatment strategies differ based on the etiology.[10,11] However, regardless of stricture type, all carry a risk of progressing to clinical adverse outcomes (CAO) during disease progression.

Received: 25 March 2025
Accepted: 25 July 2025
Published: 8 August 2025

Inflammatory strictures arise from intestinal edema and localized inflammation induced by transmural inflammation and are often responsive to medical therapy with corticosteroids or anti-TNF agents. Conversely, fibrotic strictures result from irreversible fibrotic scarring. Due to a lack of proven medical treatments, they require endoscopic dilation or surgery. Endoscopic dilation offers transient symptom relief but carries risks of perforation and recurrence. Surgical resection, though definitive, may cause short bowel syndrome and disease relapse. Despite these limitations, timely stratification of CD strictures to identify high-risk patients is critical. Early personalized intervention can significantly alter long-term disease outcomes.

Cross-sectional imaging and endoscopy are primary diagnostic tools for CD strictures, essential for clinical diagnosis and management.[10] Computed tomography enterography (CTE), magnetic resonance enterography (MRE), and intestinal ultrasound provide detailed views of intestinal structure and lesions.[8,12,13] However, the accuracy of these tools can be affected by subjective interpretation and the clinician's experience. Radiomics, a field that analyzes vast amounts of imaging data, is finding increasing use in CD research.[14–18] The absence of standardized criteria for defining intestinal strictures on cross-sectional imaging compromises diagnostic consistency and accuracy. Conversely, endoscopy provides direct visualization of the intestinal lumen, enabling precise assessment of luminal narrowing. Endoscopic strictures were defined as DBE impassable or diameter <10 mm.[19]

To our knowledge, there are few studies reported on using radiomics features to predict clinical outcomes in patients with stricturing CD. Li et al[8] and Chaudhry et al[20] reported that CD patients with bowel strictures identified on cross-sectional imaging were at increased risk of developing CAO. However, their study did not further stratify these patients based on imaging characteristics to identify high-risk subgroups. Similarly, while previous studies associate obstructive symptoms, disease duration, and stricture length with surgical intervention need,[13,21] and link stricture length to adalimumab efficacy,[10] they did not further explore the potential of radiomics signatures in predicting GAO.

Therefore, this study aims to combine clinical features with radiomics features to develop a nomogram model, predicting the risk of CAO in patients with stricturing CD. This research could aid clinicians in stratifying CD patients by risk, timely identifying those at high risk, and implementing close monitoring and intervention measures, thereby improving patients' long-term prognoses.

Materials and Methods

Patient Population

This retrospective study was conducted at The First Affiliated Hospital of Anhui Medical University and was approved by the Institutional Review Board, with patient informed consent being waived. We collected data from patients with CD who were treated at our hospital from January 2018 to March 2023. The diagnosis of CD conformed to the diagnostic guidelines of the European Crohn's and Colitis Organization (ECCO). The inclusion criteria were as follows: (1) age of onset over 14 years; (2) patients who underwent both endoscopy and CTE examination within three days at baseline; (3) intestinal lesions that could be reached by endoscopy, meeting the definition of endoscopic stenosis; (4) patients with intestinal strictures who had not undergone endoscopic dilation at baseline; (5) complete clinical data available and during follow-up; (6) a minimum follow-up period of three months. The exclusion criteria were as follows: (1) poor quality of CTE images; (2) concurrent penetrating disease at baseline; (3) patients with intestinal tumors or other infectious disease; (4) patients with anastomotic strictures. A total of 219 patients met these criteria and were included (Figure 1). Patients were randomly assigned to a training set (n=153) and a testing set (n=66) in a 7:3 ratio. Clinical baseline data recorded included gender, age, duration of disease, Body Mass Index (BMI), disease location, C-reactive protein (CRP), Erythrocyte sedimentation rate (ESR), Hemoglobin (Hb), Albumin (Alb), Platelet (PLT), Harvey-Bradshaw Index (HBI), perianal disease, and concomitant treatment. The disease duration was defined from the initial diagnosis to the detection of intestinal stricture. An HBI≤4 indicated remission, while >4 suggested active disease. Concomitant treatment primarily included 5-aminosalicylic acid, steroids, immunosuppressants, and anti-TNF antibodies.

CTE Examination and Radiological Assessment

All patients underwent standardized bowel preparation before the CTE examination. The procedure included a 12-hour fast to ensure adequate bowel cleanliness. Patients orally ingested 500 mL of an isotonic solution at 45, 30, and 15 minutes before the

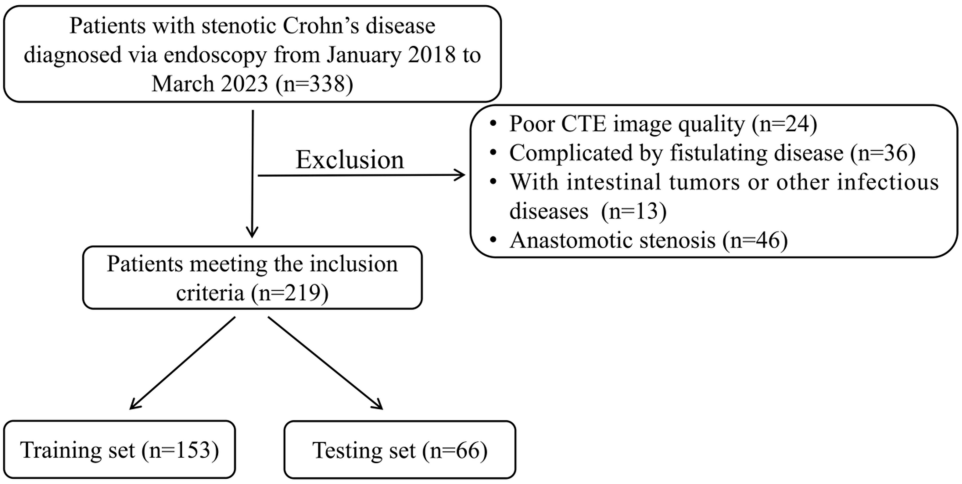

Figure 1 Flow chart of patient recruitment.

examination (a total of 1500 mL). Additionally, to reduce gastrointestinal motility-induced artifacts, 20 mg of intravenous hyoscine butylbromide was administered 10 minutes before the examination. An iodine contrast agent (320 mg/mL, 1.5mL/kg) was injected into the antecubital vein at 3.0 mL/s using a high-pressure injector. Scans were conducted using either a Revolution CT or Optima CT 680, with settings of 120 kV tube voltage, 150–300mA tube current, a 512×512 matrix, 64×0.625 detector collimation, 1.25 mm slice thickness, and 1 mm interslice gap. Data acquisition included enteric and venous phases at 45 and 70 seconds post-administration, respectively. Radiological assessments focused on the narrowed intestinal segments in CD patients, evaluating characteristics such as length of stenosis, wall thickness, upstream lumen diameter, bowel wall enhancement, comb sign, and mesenteric fat proliferation.

Double-Balloon Endoscopy Examination

All patients undergoing Double-Balloon Endoscopy (DBE) examinations were administered combined intravenous and inhalation anesthesia. The DBE utilized the EN-580T enteroscope (FUJIFILM, Tokyo, Japan) and the Overtube system, performed by three endoscopists, each with experience in over 200 IBD cases. All patients opted for the DBE examination to start rectally, with 2000 mL of polyethylene glycol electrolyte solution administered orally 4 hours before the rectal DBE for bowel preparation. The insertion depth of the DBE was calculated according to the method described in previous literature.[22] DBE-related stenosis in CD was defined as the inability to pass through the endoscope or an internal diameter of the small intestine of less than 10 mm.[23]

Matching and Recording of the Location of CTE and Endoscopic Strictures

In the CTE examination: The ileum, starting from the ileocecal valve, is divided into four sections, each 20 cm in length. According to the Lémann index,[19] these four sections are sequentially recorded as ileum 1, ileum 2, ileum 3, ileum 4. In the endoscopic examination: A DBE via the anal route is performed to detect intestinal stenosis. The localization of ileal stenosis is determined based on the distance from the ileocecal valve.

Baseline, Follow-up Endpoint, and Clinical Adverse Outcomes

The baseline time is defined as the time when intestinal stenosis is first detected endoscopically. The follow-up endpoint is defined as the time when the targeted intestinal stenosis leads to a CAO. Clinical adverse outcomes of intestinal stenosis include the following scenarios: (1) stenosis-related surgery (including bowel resection or strictureplasty), confirmed by reviewing medical records, telephone follow-ups, etc.; (2) the new onset of penetrating disease, such as fistulas, sinus tracts, abscesses, or intestinal perforation, acute intestinal obstruction, or retention of the capsule endoscope, confirmed through endoscopic examination or cross-sectional imaging during the follow-up period. For intestinal stenoses that did not result in clinical adverse outcomes, the follow-up endpoint is set to December 31, 2023.

Establishing a Radiomics Nomogram Model to Predict Clinical Adverse Outcomes

The establishment of the radiomics model are shown in the Supplementary Methods and Figure S1. We utilized univariate Cox regression analysis to compare the difference in clinical risk factors between two groups in the training set. Variables that achieved $P<0.1$ in the univariate Cox regression were entered into the multivariable Cox regression, together with sex, age and BMI, which were forced into the model regardless of their univariate significance, to construct the final clinical model ($P<0.05$). The hazard ratio (HR) for each independent risk factor was calculated as an estimate of relative risk, with a 95% confidence interval (CI). The optimal cutoff values for clinical risk factors (continuous variables) were determined using X-tile software (version 3.6.1, Rimm Lab, Yale School of Medicine) to explore whether clinical risk factors were associated with clinical adverse outcomes.

In the training set, patients were divided into low- and high-risk groups based on their Rad-score, with the optimal cutoff value determined using X-tile software; the same Rad-score cutoff value was used in the testing set. Kaplan–Meier survival analysis was employed to investigate whether the Rad-score in each cohort was associated with clinical adverse outcomes. A radiomics nomogram model combining clinical risk factors with the Rad-score was established to predict clinical adverse outcomes in CD with strictures. The performance of the radiomics nomogram model was evaluated using time-dependent Receiver Operating Characteristic (ROC) curves, plotting ROC curves for 1-year, 2-year, and 3-year, and calculating the Area Under the Curve (AUC). Additionally, Harrell's concordance index (C-index) was calculated to assess the performance of the radiomics nomogram model, and calibration curves were plotted to evaluate the accuracy of the model.

Furthermore, Decision Curve Analysis (DCA) was conducted to quantify the net benefits at different threshold probabilities, assessing the clinical effectiveness of the model. We also calculated the Net Reclassification Improvement (NRI) and Integrated Discrimination Improvement (IDI) to compare the predictive value-added between the nomogram and the clinical model.

Statistical Analysis

Continuous variables following a normal distribution will be expressed as mean ± standard deviation and compared using the independent sample *t*-test. For variables not conforming to a normal distribution, the median and its interquartile range will be used for expression, and the Mann–Whitney *U*-test will be applied for intergroup comparisons. Differences between categorical variables will be compared using the Chi-square test or Fisher's exact test. In univariate Cox regression analysis, variables with $P<0.1$ will be included in the multivariable Cox regression analysis to screen for independent prognostic factors for clinical adverse outcomes. The X-tile software will be used to calculate the optimal cutoff values for clinical features and the Rad-score (The optimal cutoff was determined exclusively from the training cohort to maximize discrimination of adverse outcome risk. This fixed threshold was then applied to the test cohort for validation, ensuring unbiased assessment of its prognostic stability). Kaplan–Meier curve analysis will be used to compare clinical adverse outcomes among different risk stratification subgroups, with subgroup comparisons made using the Log rank test. Statistical analyses will be conducted using SPSS (version 25.0) and R software (version 3.5.3, http://www.r-project.org). A two-sided $P<0.05$ will be considered statistically significant.

Results

General Characteristics of Patients

The clinical characteristics of the 219 enrolled patients are presented in Table 1, with 72 patients experiencing clinical adverse outcomes, including 50 in the training set and 22 in the testing set. The training set consisted of 153 patients, including 99 males and 54 females; the average age was 38.3 years; the median duration of the disease was 24 months; the average BMI was 20.3. In the testing set, there were 66 patients, including 50 males and 16 females; the average age was 36.6 years; the median duration of the disease was 26 months; the average BMI was 20.5. The CTE radiological characteristics of the patients are detailed in Table 2.

Table 1 Demographic and Clinical Characteristics of Patient with Crohn's Disease

Characteristics	Training (n=153)	Testing (n=66)	*P* Value
Sex (male/female, n)	99/54	50/16	0.108
Age, years (mean±SD)	38.3±12.7	36.6±11.7	0.336
Duration of the disease, months, median (IQR)	24 (12–72)	26 (12–72)	0.790
BMI, kg/m^2 (mean±SD)	20.3±1.6	20.5±2.1	0.349
Disease location, n (%)			0.186
L1 (Ileal)	64 (41.8%)	34 (51.5%)	
L2 (Colonic)	0 (0%)	0 (0%)	
L3 (Ileocolonic)	89 (58.2%)	32 (48.5%)	
CRP, mg/L, median (IQR)	3.9 (1.3–14.9)	4.5 (2.1–16.7)	0.292
ESR, mm/h, median (IQR)	21 (10–31.5)	24.5 (12–36)	0.270
Hb, g/L, median (IQR)	119 (104–134)	126 (112–136)	0.076
Alb, g/L, median (IQR)	37.4 (34.7–40.3)	37.7 (33.2–41.4)	0.994
PLT, ×109/L, median (IQR)	264 (205–328)	256.5 (191–300)	0.520
HBI, n (%)			0.342
Activity	94 (61.4%)	45 (68.2%)	
Remission	59 (38.6%)	21 (31.8%)	
Perianal involvement, n (%)			0.279
Yes	40 (26.1%)	22 (33.3%)	
No	113 (73.9%)	44 (66.7%)	
Concomitant treatments, n (%)			
5-ASA	10 (6.5%)	6 (9.1%)	0.505
Steroids	21 (13.7%)	12 (18.2%)	0.398
Immunosuppressants	41 (26.8%)	12 (18.2%)	0.172
Anti-TNF antibodies	93 (60.8%)	47 (71.2%)	0.140
Clinical adverse outcome			0.925
Yes	50 (32.7%)	22 (33.3%)	
No	103 (67.3%)	44 (66.7%)	

Notes: Data following a normal distribution are shown as the mean ± SD, while those not normally distributed are depicted as median (IQR) and categorical variables are displayed as count (%).

Abbreviations: BMI, Body Mass Index; SD, Standard Deviation; IQR, Interquartile Range; CRP, C reactive protein; ESR, Erythrocyte sedimentation rate; Hb, Hemoglobin; Alb, Albumin; PLT, Platelet; HBI, Harvey-Bradshaw Index; 5-ASA, 5-Aminosalicylic Acid; TNF, Tumor Necrosis Factor.

Table 2 Radiological Characteristics in CTE Images of Patients with Crohn's Disease

Radiological Characteristics	Training (n=153)	Testing (n=66)	*P* Value
Stricture length, mm (mean±SD)	63.8±35.3	58.5±24.1	0.271
Bowel wall thickness, mm (mean±SD)	5.4±1.5	5.5±1.6	0.228
Diameter of upstream lumen, mm (mean±SD)	31.1±9.8	30.2±8.9	0.526
Hyperenhancement, n (%)			0.805
Yes	90 (58.8%)	40 (60.6%)	
No	63 (41.2%)	26 (39.4%)	
Comb sign, n (%)			0.586
Yes	75 (49.0%)	35 (53.0%)	
No	78 (51.0%)	31 (47.0%)	
Fibrofatty proliferation, n (%)			0.951
Yes	106 (69.3%)	46 (69.7%)	
No	47 (30.7%)	20 (30.3)	

Notes: Data following a normal distribution are shown as the mean ± SD, while those not normally distributed are depicted as median (IQR) and categorical variables are displayed as count (%).

Abbreviations: CTE, Computed Tomography Enterography; SD, Standard Deviation.

Establishment of the Clinical Model

Univariate Cox regression analysis of clinical variables in the training set showed that disease location (P=0.030), HBI (P=0.001), perianal involvement (P=0.059), and diameter of the upstream lumen (P<0.001) demonstrated significant statistical differences in predicting clinical adverse outcomes. Subsequent multivariate Cox regression analysis further indicated that HBI (HR=0.456, 95% CI=0.217–0.975, P=0.038) and diameter of the upstream lumen (HR=1.081, 95% CI=1.050–1.113, P<0.001) could serve as independent predictors of clinical adverse outcomes in the clinical model, as detailed in Table 3. Using the X-tile tool, the optimal cutoff value for the diameter of the upstream lumen was determined to be 35 mm. Based on this threshold, patients were divided into two groups: those with a diameter of the upstream lumen ≤35 mm and those with a diameter of the upstream lumen >35 mm. Kaplan–Meier survival analysis further confirmed significant differences in the incidence of clinical adverse outcomes between the two groups defined by HBI scores (active phase versus remission phase) and between the groups with a diameter of the upstream lumen ≤35 mm versus >35 mm, as shown in Figures 2 and 3, respectively.

Establishment of the Radiomics Nomogram Model

Among the clinical and radiological characteristics, the HBI score and the diameter of the upstream lumen were identified as independent predictors of clinical adverse outcomes in patients with CD with strictures. Radiomics model development results are shown in the Supplementary Results. These predictors were combined with the Rad-score to establish a radiomics nomogram model, and a nomogram was derived based on the training set, as shown in Figure 4.

Table 3 Univariate and Multivariate Cox Regression of Clinical Variables

Clinical Variables	Univariate Cox Regression		Multivariate Cox Regression	
	HR (95% CI)	*P* Value	HR (95% CI)	*P* Value
Sex	0.673 (0.363–1.249)	0.209	0.872 (0.450–1.688)	0.684
Age	1.008 (0.987–1.030)	0.447	1.016 (0.993–1.039)	0.180
Duration of the disease	1.001 (0.997–1.006)	0.649	NA	NA
BMI	1.067 (0.911–1.250)	0.422	1.091 (0.917–1.299)	0.326
Disease location	1.850 (1.060–3.226)	0.030	1.412 (0.781–2.553)	0.253
CRP	0.995 (0.978–1.011)	0.515	NA	NA
ESR	0.999 (0.983–1.015)	0.871	NA	NA
Hb	1.010 (0.996–1.024)	0.157	NA	NA
Alb	1.055 (0.986–1.129)	0.120	NA	NA
PLT	0.997 (0.994–1.001)	0.120	NA	NA
HBI	0.302 (0.146–0.621)	0.001	0.456 (0.217–0.957)	0.038*
Perianal involvement	2.073 (0.973–4.418)	0.059	1.820 (0.740–4.430)	0.190
5-ASA	1.528 (0.371–6.291)	0.557	NA	NA
Steroids	2.096 (0.754–5.826)	0.156	NA	NA
Immunosuppressants	1.227 (0.641–2.349)	0.537	NA	NA
Anti-TNF antibodies	1.156 (0.659–2.027)	0.613	NA	NA
Stricture length	1.001 (0.993–1.009)	0.795	NA	NA
Bowel wall thickness	0.974 (0.807–1.176)	0.786	NA	NA
Diameter of upstream lumen	1.075 (1.050–1.100)	< 0.001	1.081 (1.050–1.113)	< 0.001*
Hyperenhancement	1.140 (0.652–1.993)	0.646	NA	NA
Comb sign	1.075 (0.617–1.872)	0.799	NA	NA
Fibrofatty proliferation	1.426 (0.800–2.544)	0.229	NA	NA

Notes: *P<0.05.

Abbreviations: HR, Hazard Ratio; CI, Confidence Interval; NA, Not Applicable; BMI, Body Mass Index; CRP, C reactive protein; ESR, Erythrocyte sedimentation rate; Hb, Hemoglobin; Alb, Albumin; PLT, Platelet; HBI, Harvey-Bradshaw Index; 5-ASA, 5-Aminosalicylic Acid; TNF, Tumor Necrosis Factor. Table 4: C-index, Concordance index; AUC, Area Under the Curve; CI, Confidence Interval.

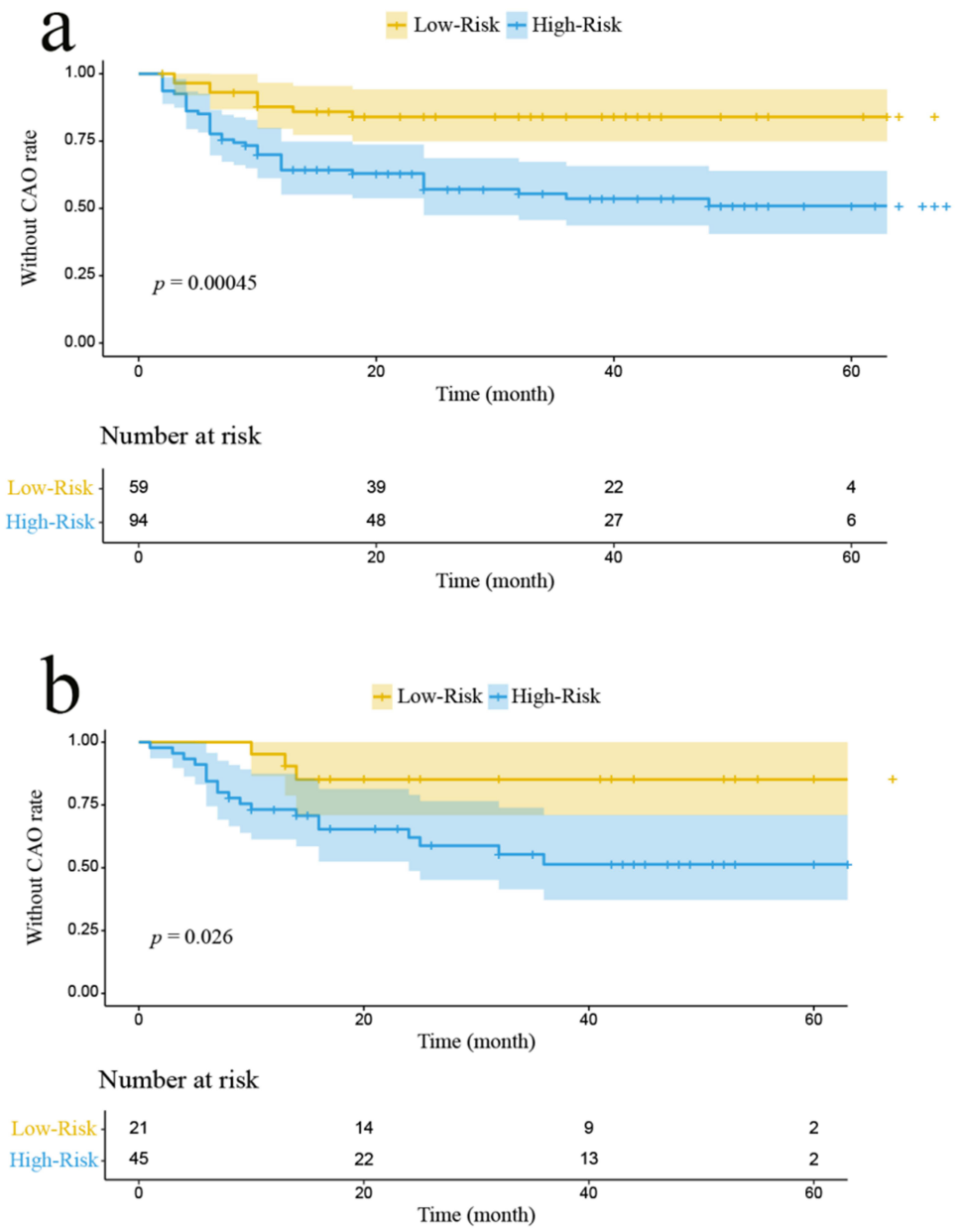

Figure 2 In the training (**a**) and testing set (**b**), Kaplan–Meier curves of patients stratified by different risks based on HBI scores for clinical adverse outcomes.

Performance Evaluation of the Clinical Model, Radiomics Model, and Nomogram Model

In the training set, compared with the clinical model (C-index 0.764; 1-year AUC = 0.790; 2-year AUC = 0.833; 3-year AUC = 0.862), the radiomics model achieved a higher C-index of 0.813 (ΔC-index = 0.049; 1-year AUC = 0.793; 2-year AUC = 0.887; 3-year AUC = 0.929), while the integrated radiomics nomogram further increased the C-index to 0.848 (ΔC-index = 0.084; 1-year AUC = 0.890; 2-year AUC = 0.928; 3-year AUC = 0.955), demonstrating progressively improved discrimination of CAO in CD patients with strictures. Similar results were observed in the testing set (Table 4 and Figure 5). The calibration curves of the nomogram model in both the training and testing sets demonstrated good agreement between predicted and observed risks (Figure 6). In the training set, the calibration slopes (intercepts) for 1-, 2-, and 3-year predictions were 0.65 (−0.52), 0.87 (0.20), and 1.07 (1.07), respectively. In the testing set, the corresponding values were 0.70 (−0.48), 0.62 (0.49), and 1.15 (2.18), indicating only minor systematic bias. DCA (Figure S2) further showed that, in the training set, the nomogram delivered a positive net benefit across threshold

https://doi.org/10.2147/JIR.S526700

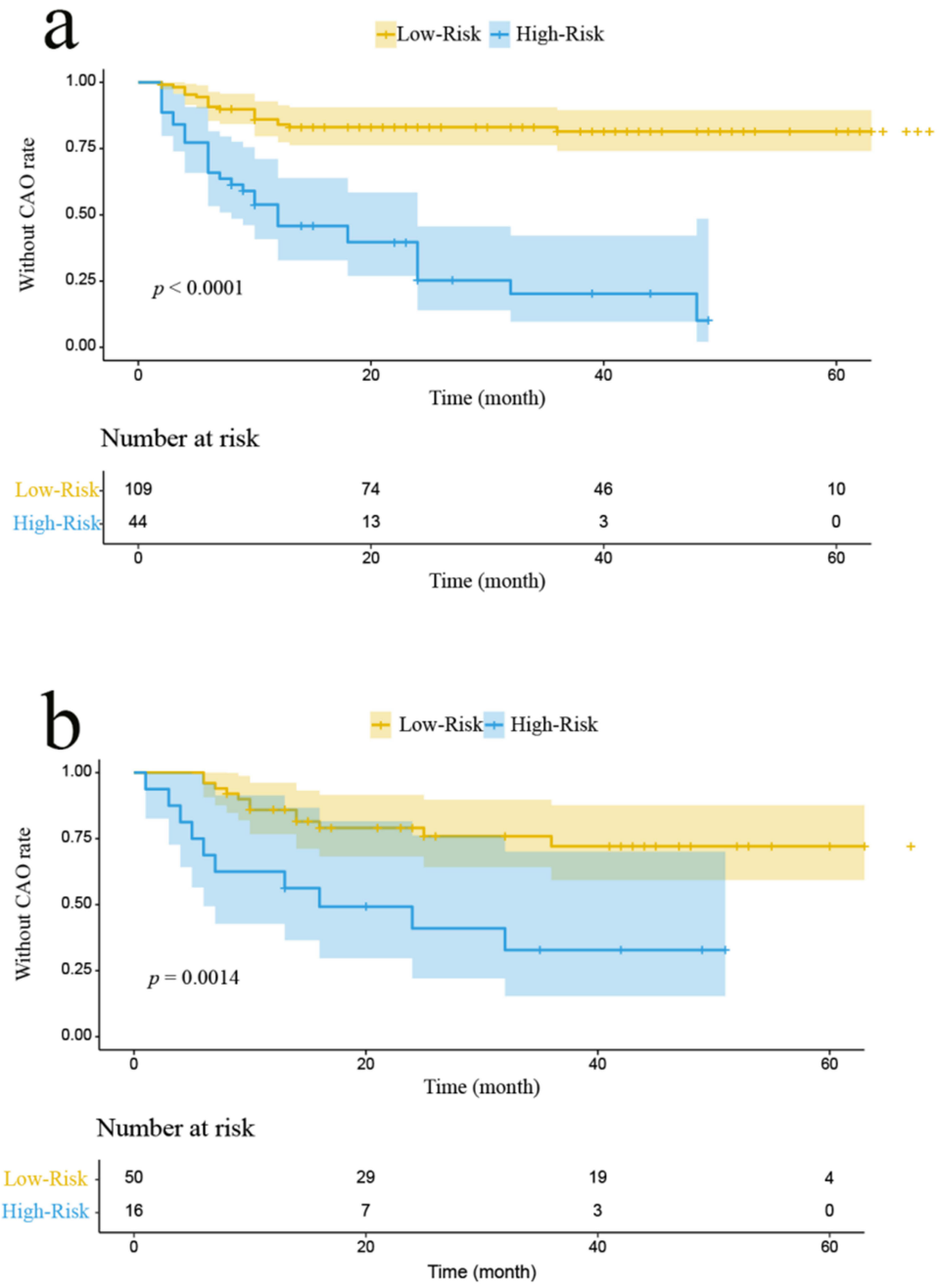

Figure 3 In the training (**a**) and testing set (**b**), Kaplan–Meier curves of patients stratified by different risks based on the diameter of the upstream lumen for clinical adverse outcomes.

probabilities of 0.01–0.83, out performing the clinical model (0.10–0.76) and the radiomics-only model (0.03–0.99) over most of this range. In the testing sets, the nomogram remained advantageous between 0.01 and 0.76, whereas the clinical and radiomics models were beneficial within narrower windows of 0.15–0.50 and 0.08–0.71, respectively. These findings confirm both the reliable calibration and the superior clinical utility of the proposed nomogram.

In the training set, the nomogram model achieved an NRI of 0.475 (95% CI, 0.309–0.699, $P<0.05$) and an IDI of 0.197 (95% CI, 0.134–0.286, $P<0.05$) compared to the clinical model; in the testing set, the NRI was 0.557 (95% CI, 0.060–0.732, $P<0.05$) and the IDI was 0.206 (95% CI, 0.011–0.486, $P<0.05$) compared to the clinical model.

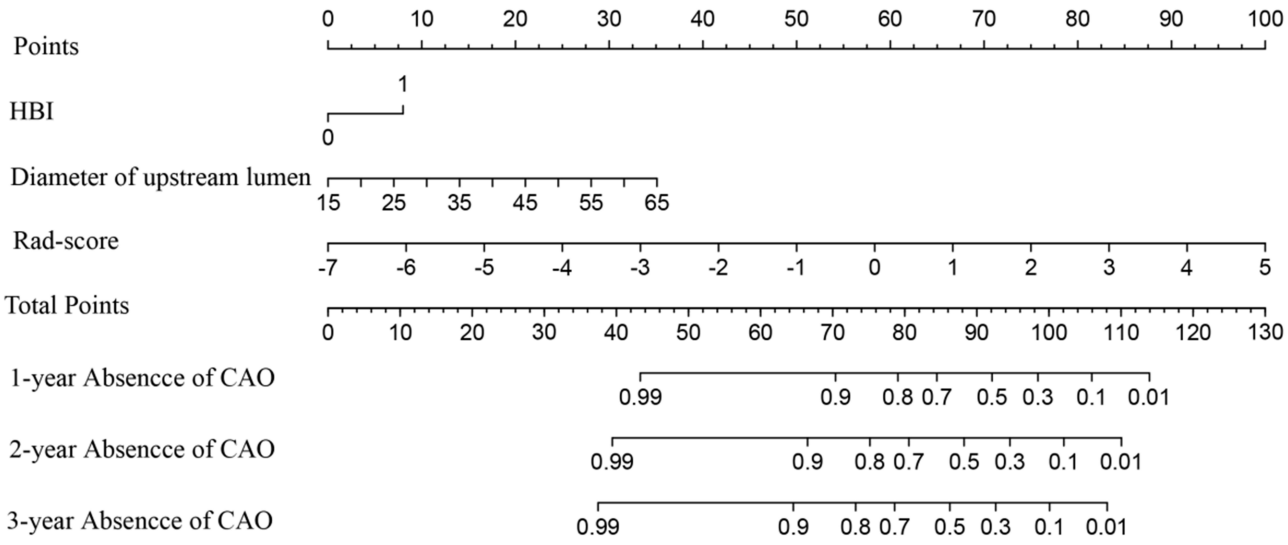

Figure 4 The clinical radiomics nomogram constructed using clinical variables and Rad-score to assess the risk of clinical adverse outcomes in patients with stricturing Crohn's disease.

Discussion

Our study highlights significant advancements in the use of radiomics for predicting clinical adverse outcomes in patients with stricturing Crohn's disease (CD). We have demonstrated that radiomics features, extracted from endoscopically assessed strictured bowel segments, can effectively predict clinical adverse outcomes, showing high discriminative ability.

Currently, there are no validated non-invasive biomarkers for predicting clinical adverse outcomes in patients with stricturing CD. This study seeks to predict the prognosis of CD based on clinical characteristics and radiological findings. Previous research suggests that obstructive symptoms, disease duration, and stricture length are indicative of the need for surgical intervention,[13,21] with stricture length also linked to the efficacy of adalimumab treatment.[10] However, our study did not use stricture length as a predictive factor, possibility due to differences in patient samples confirmed by endoscopic examination. Unlike studies utilizing cross-sectional imaging for stricture identification, our cohort specifically comprised patients with endoscopically confirmed stricturing Crohn's disease. In our study, disease duration emerged as a more valuable predictor. We propose that prolonged disease course correlates with increased likelihood of intestinal fibrosis progression, consequently leading to poorer stricture prognosis—a finding consistent with prior research.[13] In stricturing Crohn's disease, CAO strongly correlate with disease activity. Our study observed significantly elevated CAO risk during active phases. This association stems from multifactorial mechanisms: exacerbated inflammation driving intestinal lesion progression, immune dysregulation heightening infection susceptibility, suboptimal therapeutic responses due to inadequate dosing or drug resistance, and psychosocial comorbidities modulating immune-inflammatory pathways—collectively worsening prognosis. We also observed that upstream luminal diameter significantly correlates with CAO in stricturing Crohn's disease patients. Greater upstream dilatation typically reflects more severe strictures and predisposes to CAO development, consistent with the findings of Li et al.[8] Our study demonstrated that the nomogram model outperformed both clinical and radiomics models alone, highlighting the incremental value of radiomics features in predicting stricturing Crohn's disease prognosis. By integrating clinical factors with radiomics characteristics, the nomogram provides a comprehensive assessment of patient status, enabling more accurate predictions to guide personalized treatment plans and management strategies. Our study explores radiomics' potential in predicting CAO in patients with stricturing CD, thus broadening its scope of investigation. Previously, research primarily focused on using radiomics for CD diagnosis, disease activity assessment and prognosis.[24–28]

Lesion annotation in radiomics research is arduous and time-intensive, particularly in complex diseases like CD, where selecting appropriate annotations is challenging. Historically, studies have relied on manual segmentation,

Table 4 Performance of the Clinical Model, Radiomics Model, and Nomogram Model in the Training and Testing Sets

Model	Training				Testing			
	C-index (95% CI)	1 year AUC (95% CI)	2 year AUC (95% CI)	3 year AUC (95% CI)	C-index (95% CI)	1 year AUC (95% CI)	2 year AUC (95% CI)	3 year AUC (95% CI)
Clinical	0.764 (0.704, 0.824)	0.790 (0.706, 0.874)	0.833 (0.755, 0.913)	0.862 (0.789, 0.936)	0.752 (0.649, 0.854)	0.741 (0.603, 0.880)	0.748 (0.603, 0.894)	0.816 (0.678, 0.954)
Radiomics	0.813 (0.764, 0.862)	0.854 (0.793, 0.916)	0.887 (0.828, 0.946)	0.929 (0.878, 0.981)	0.775 (0.667, 0.882)	0.818 (0.671, 0.964)	0.811 (0.680, 0.942)	0.906 (0.810, 1.000)
Nomogram	0.848 (0.805, 0.891)	0.890 (0.833, 0.946)	0.928 (0.880, 0.976)	0.955 (0.917, 0.994)	0.849 (0.765, 0.933)	0.874 (0.756, 0.993)	0.863 (0.751, 0.975)	0.956 (0.892, 1.000)

Abbreviations: C-index, Concordance index; AUC, Area Under the Curve; CI, Confidence Interval.

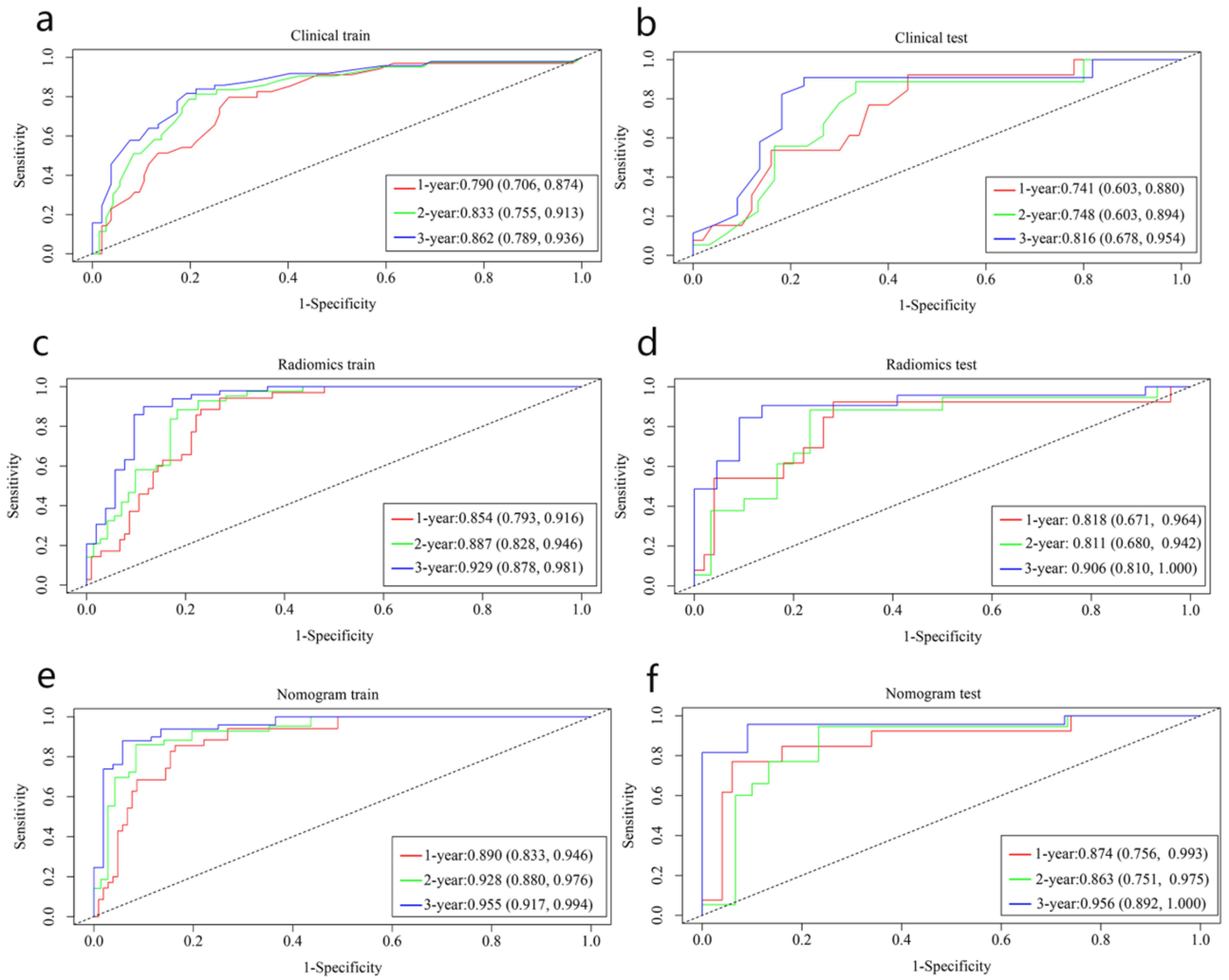

Figure 5 Time-dependent ROC curves, where parts (**a**) (training set) and (**b**) (testing set) represent the clinical model, parts (**c**) (training set) and (**d**) (testing set) illustrate the radiomics model, and parts (**e**) (training set) and (**f**) (testing set) showcase the nomogram model.

requiring significant time and manpower. Although we developed an automatic segmentation model that performed well in prior research with a Dice Similarity Coefficient (DSC) of 0.824,[29] we did not employ this model in the current study focused on strictured intestinal segments in CD. Our model, capable of segmenting all lesions in CD patients' CTE images, was not used because we wanted to specifically target strictured segments. However, we plan to refine this model to more precisely identify strictured segments in future studies, aiming to enhance its utility in diagnosing and managing stricturing CD. Although an automatic segmentation model was not employed, favorable inter- and intra-observer consistency results support the reliability of feature extraction.

Our study is limited by several factors. Firstly, the small sample size and single center nature of the study might lead to sample selection bias and limit the generalizability of our findings. Validation in a larger, more diverse population is necessary to confirm our results. Additionally, the retrospective design may compromise data completeness and accuracy. Another limitation is that small bowel endoscopy does not cover the entire intestine, which may miss some small bowel strictures, potentially affecting our findings. Solitano et al demonstrated that relying solely on endoscopy may miss stricturing disease in one-third of cases, with these missed cases later identified on cross-sectional imaging.[30] However, it should be noted that radiological strictures do not fully correspond to endoscopic strictures. If all stenoses found on cross-sectional imaging were also taken into account in our study, the role of radiomics in the nomogram would be greatly enhanced, although we did not further analyze this situation. The use of 3D segmentation for annotating strictured

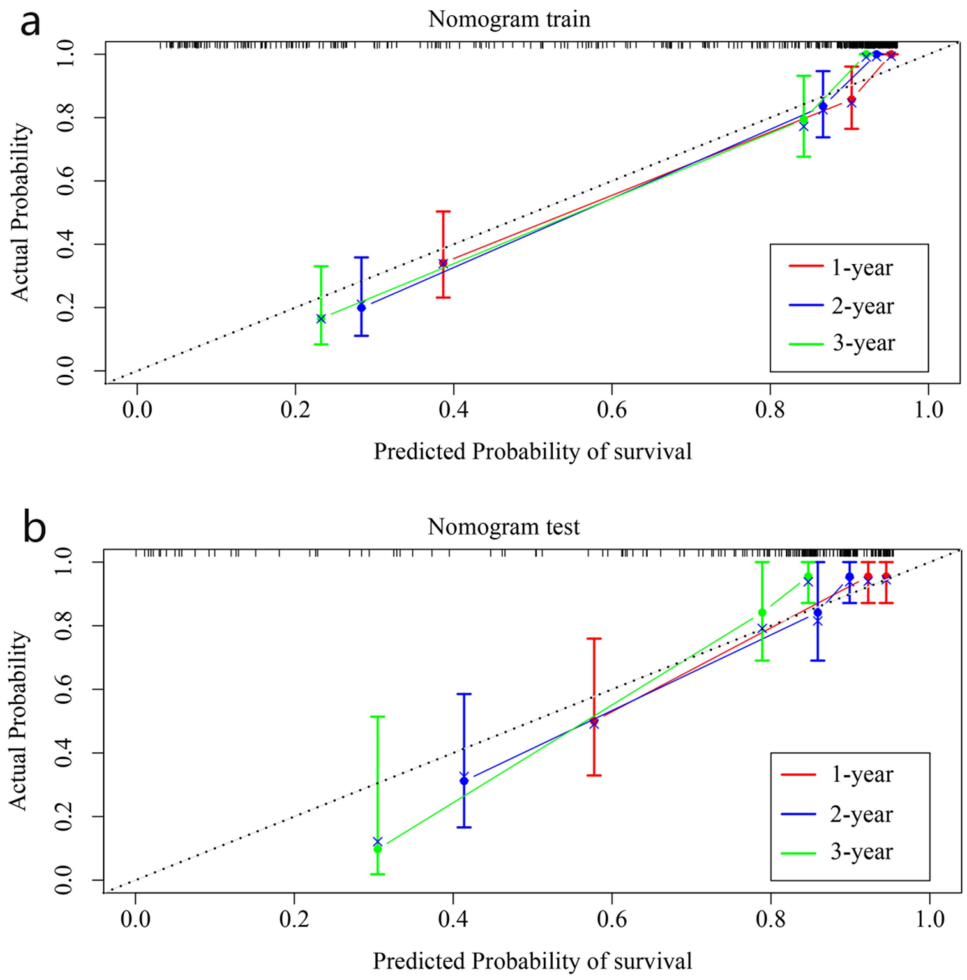

Figure 6 Demonstrates the calibration of the nomogram model in the training (**a**) and the testing set (**b**), regarding the agreement between predicted and observed outcomes of no adverse clinical events at 1 year, 2 years, and 3 years.

segments is also time-intensive. Future work focus on developing deep learning models for automatic segmentation, which would increase efficiency and minimize human error. Furthermore, this study focused solely on the radiomics features of strictured segments and did not include those of non-strictured bowel lesions, visceral fat, or mesenteric tissues. Accurate segmentation of these areas is time consuming and could reduce clinical practicality. Expanding the scope to include these features in future studies could improve the predictive performance for clinical adverse outcomes in CD. Lastly, while radiomics features have been promising in various studies, their biological significance and interpretability remain limited. Future research is needed to explore these aspects to better inform clinical decisions and personalized treatment strategies.

Conclusion

In summary, this retrospective study demonstrates that radiomics features derived from CTE of endoscopically confirmed strictured bowel segments in Crohn's disease CD patients correlate with clinical adverse outcomes. These findings highlight the potential of radiomics signatures as non-invasive predictors for prognostic stratification in stricturing CD.

Abbreviations

CTE, Computed tomography enterography; CAO, Clinical adverse outcomes; CD, Crohn's disease; LASSO, Least absolute shrinkage and selection operator; Index, Harrell's concordance index; ROC, Receiver operating characteristic; DCA, Decision

curve analysis; IBD, Inflammatory bowel disease; UC, Ulcerative colitis; MRE, Magnetic resonance enterography; ECCO, European Crohn's and Colitis Organization; DBE, Double-Balloon Endoscopy; HR, Hazard ratio; CI, Confidence interval; AUC, Area under the curve; NRI, Net reclassification improvement; IDI, Integrated discrimination improvement.

Ethical Statement

The authors are accountable for all aspects of the work in ensuring that questions related to the accuracy or integrity of any part of the work are appropriately investigated and resolved. The study was conducted in accordance with the Declaration of Helsinki (as revised in 2013) and was approved by the First Affiliated Hospital of Anhui Medical University Ethics Committee (No. PJ 2024-11-68). The ethics committee waived informed consent requirements for this purely retrospective study analyzing pre-existing anonymized medical imaging data, based on implementation of rigorous anonymization protocols, compliance with Declaration of Helsinki Article 32 governing retrospective data use, and confirmation of no patient welfare risks.

Funding

There is no funding to report.

Disclosure

The authors report no conflicts of interest in this work.

References

1. Ng SC, Shi HY, Hamidi N, et al. Worldwide incidence and prevalence of inflammatory bowel disease in the 21st century: a systematic review of population-based studies [published correction appears in Lancet. *Lancet*. 2020;396(10256):e56. doi:10.1016/S0140-6736(17)32448-0
2. Hordonneau C, Buisson A, Scanzi J, et al. Diffusion-weighted magnetic resonance imaging in ileocolonic Crohn's disease: validation of quantitative index of activity. *Am J Gastroenterol*. 2014;109(1):89–98. doi:10.1038/ajg.2013.385
3. Cosnes J, Gower-Rousseau C, Seksik P, et al. Epidemiology and natural history of inflammatory bowel diseases. *Gastroenterology*. 2011;140(6):1785–1794. doi:10.1053/j.gastro.2011.01.055
4. Thia KT, Sandborn WJ, Harmsen WS, et al. Risk factors associated with progression to intestinal complications of Crohn's disease in a population-based cohort. *Gastroenterology*. 2010;139(4):1147–1155. doi:10.1053/j.gastro.2010.06.070
5. Rieder F, Bettenworth D, Ma C, et al. An expert consensus to standardise definitions, diagnosis and treatment targets for anti-fibrotic stricture therapies in Crohn's disease. *Aliment Pharmacol Ther*. 2018;48(3):347–357. doi:10.1111/apt.14853
6. Rieder F, Zimmermann EM, Remzi FH, et al. Crohn's disease complicated by strictures: a systematic review. *Gut*. 2013;62(7):1072–1084. doi:10.1136/gutjnl-2012-304353
7. Freeman HJ. Natural history and long-term clinical course of Crohn's disease. *World J Gastroenterol*. 2014;20(1):31–36. doi:10.3748/wjg.v20.i1.31
8. Shi L, Wang YD, Shen XD, et al. Clinical outcome is distinct between radiological stricture and endoscopic stricture in ileal Crohn's disease. *Eur Radiol*. 2023;33(11):7595–7608. doi:10.1007/s00330-023-09743-5
9. Gearry RB, Kamm MA, Hart AL, et al. Predictors for developing intestinal failure in patients with 'Crohn's disease. *J Gastroenterol Hepatol*. 2013;28(5):801–807. doi:10.1111/jgh.12115
10. Bouhnik Y, Carbonnel F, Laharie D, et al. Efficacy of Adalimumab in patients with Crohn's disease and symptomatic small bowel stricture: a multicentre, prospective, observational cohort (CREOLE) study. *Gut*. 2018;67(1):53–60. doi:10.1136/gutjnl-2016-312581
11. Rieder F, Fiocchi C, Rogler G. Mechanisms, management, and treatment of fibrosis in patients with inflammatory bowel diseases. *Gastroenterology*. 2017;152(2):340–350.e346. doi:10.1053/j.gastro.2016.09.047
12. Pal P, Gala J, Rebala P, et al. Re-intervention rates and symptom-free survival at 1 year after endoscopic versus surgical management of strictures in Crohn's disease: a propensity matched analysis of a prospective inflammatory bowel disease cohort. *J Gastroenterol Hepatol*. 2024;39(2):353–359. doi:10.1111/jgh.16384
13. El Ouali S, Baker ME, Lyu R, et al. Validation of stricture length, duration and obstructive symptoms as predictors for intervention in ileal stricturing Crohn's disease. *United Eur Gastroenterol J*. 2022;10(9):958–972. doi:10.1002/ueg2.12314
14. Lambin P, Rios-Velazquez E, Leijenaar R, et al. Radiomics: extracting more information from medical images using advanced feature analysis. *Eur J Cancer*. 2012;48(4):441–446. doi:10.1016/j.ejca.2011.11.036
15. Liu RX, Li H, Towbin AJ, et al. Machine learning diagnosis of small-bowel Crohn disease using t2-weighted mri radiomic and clinical data. *AJR Am J Roentgenol*. 2024;222(1):e2329812. doi:10.2214/ajr.23.29812
16. Gong T, Li M, Pu H, et al. Computed tomography enterography-based multiregional radiomics model for differential diagnosis of Crohn's disease from intestinal tuberculosis. *Abdom Radiol*. 2023;48(6):1900–1910. doi:10.2214/ajr.23.29812
17. Li H, Mo Y, Huang C, et al. An MSCT-based radiomics nomogram combined with clinical factors can identify Crohn's disease and ulcerative colitis. *Ann Transl Med*. 2021;9(7):572. doi:10.21037/atm-21-1023
18. Li X, Zhang N, Hu C, et al. CT-based radiomics signature of visceral adipose tissue for prediction of disease progression in patients with Crohn's disease: a multicentre cohort study. *EClinicalMedicine*. 2023;56(101805). doi:10.1016/j.eclinm.2022.101805
19. Pariente B, Torres J, Burisch J, et al. Validation and update of the Lemann index to measure cumulative structural bowel damage in Crohn's disease. *Gastroenterology*. 2021;161(3):853–864.e813. doi:10.1053/j.gastro.2021.05.049

20. Chaudhry NA, Riverso M, Grajo JR, et al. A fixed stricture on routine cross-sectional imaging predicts disease-related complications and adverse outcomes in patients with Crohn's disease. *Inflamm Bowel Dis*. 2017;23(4):641–649. doi:10.1097/MIB.0000000000001054
21. Lowe SC, Ream J, Hudesman D, et al. A clinical and radiographic model to predict surgery for acute small bowel obstruction in Crohn's disease. *Abdom Radiol*. 2020;45(9):2663–2668. doi:10.1007/s00261-020-02514-6
22. May A, Nachbar L, Schneider M, et al. Push-and-pull enteroscopy using the double-balloon technique: method of assessing depth of insertion and training of the enteroscopy technique using the Erlangen Endo-Trainer. *Endoscopy*. 2005;37(1):66–70. doi:10.1055/s-2004-826177
23. Navaneethan U, Vargo JJ, Menon KV, et al. Impact of balloon-assisted enteroscopy on the diagnosis and management of suspected and established small-bowel Crohn's disease. *Endosc Int Open*. 2014;2(4):E201–206. doi:10.1055/s-0034-1377522
24. Li T, Liu Y, Guo J, et al. Prediction of the activity of Crohn's disease based on CT radiomics combined with machine learning models. *J Xray Sci Technol*. 2022;30(6):1155–1168. doi:10.3233/xst-221224
25. Yao J, Zhou J, Zhong Y, et al. Computed tomography-based radiomics nomogram using machine learning for predicting one-year surgical risk after diagnosis of Crohn's disease. *Med Phys*. 2023;50(6):3862–3872. doi:10.1002/mp.16402
26. Yueying C, Jing F, Qi F, et al. Infliximab response associates with radiologic findings in bio-naive Crohn's disease. *Eur Radiol*. 2023;33(8):5247–5257. doi:10.1007/s00330-023-09542-y
27. Li X, Liang D, Meng J, et al. Development and validation of a novel computed-tomography enterography radiomic approach for characterization of intestinal fibrosis in Crohn's disease. *Gastroenterology*. 2021;160(7):2303–2316.e2311. doi:10.1053/j.gastro.2021.02.027
28. Meng J, Luo Z, Chen Z, et al. Intestinal fibrosis classification in patients with Crohn's disease using CT enterography-based deep learning: comparisons with radiomics and radiologists. *Eur Radiol*. 2022;32(12):8692–9705. doi:10.1007/s00330-022-08842-z
29. Gao Y, Zhang B, Zhao D, et al. Automatic segmentation and radiomics for identification and activity assessment of CTE lesions in Crohn's disease. *Inflamm Bowel Dis*. 2023:izad285. doi:10.1093/ibd/izad285.
30. Solitano V, Vuyyuru SK, Aruljothy A, et al. Endoscopic skipping, stricturing, and penetrating complications in crohn's disease on tandem ileo-colonoscopy and cross-sectional imaging: a retrospective cohort study [published correction appears in Inflamm Bowel Dis. 2024 Oct 01izae246. doi: 10.1093/ibd/izae246.]. *Inflamm Bowel Dis*. 2025;31(6):1529–1536. doi:10.1093/ibd/izae192